

Genetic Perturbation Alters Functional Substates in Alkaline Phosphatase

Morito Sakuma, Shingo Honda, Hiroshi Ueno, Kazuhito V. Tabata, Kentaro Miyazaki, Nobuhiko Tokuriki,* and Hiroyuki Noji*



Cite This: *J. Am. Chem. Soc.* 2023, 145, 2806–2814



Read Online

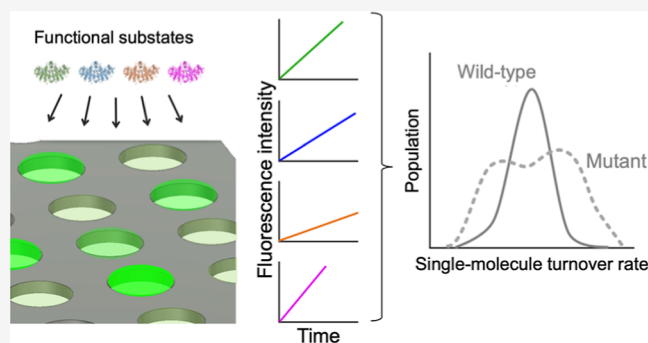
ACCESS |

Metrics & More

Article Recommendations

Supporting Information

ABSTRACT: Enzymes inherently exhibit molecule-to-molecule heterogeneity in their conformational and functional states, which is considered to be a key to the evolution of new functions. Single-molecule enzyme assays enable us to directly observe such multiple functional states or functional substates. Here, we quantitatively analyzed functional substates in the wild-type and 69 single-point mutants of *Escherichia coli* alkaline phosphatase by employing a high-throughput single-molecule assay with a femtoliter reactor array device. Interestingly, many mutant enzymes exhibited significantly heterogeneous functional substates with various types, while the wild-type enzyme showed a highly homogeneous substate. We identified a correlation between the degree of functional substates and the level of improvement in promiscuous activities. Our work provides much comprehensive evidence that the functional substates can be easily altered by mutations, and the evolution toward a new catalytic activity may involve the modulation of the functional substates.



INTRODUCTION

As our understanding of proteins matured over the years, the once simple and prevailing “one protein, one structure, one function” paradigm has undergone a substantial change. Advances in technology and statistical methods have revealed that proteins could form multiple conformational substates.^{1–4} The early studies on myoglobin gave essential contributions to the establishment of the concept that protein conformation is an ensemble of conformational substates.¹ Structural studies with X-ray crystallography, nuclear magnetic resonance (NMR), and molecular dynamics (MD) simulations also have unveiled stable conformational substates of proteins.^{5–14}

For enzymes, multiple conformational substates suggest distinct functional states, that is, functional substates. After α -lytic protease was shown to have conformational substates with distinct activity states by an elaborated biochemical study,¹⁵ it has been revealed that enzymes have multiple functional substates,^{15–28} establishing the view that enzymes are an ensemble of functional substates. Single-molecule studies have contributed to the elucidation of the functional substates. The earliest class of single-molecule kinetic assay with fluorogenic substrate revealed that enzymes show dynamic transitions between functional states, termed dynamic disorder.^{17,21} Highly parallel single-molecule enzymatic assays such as femtoliter droplet array device (FRAD) or relevant systems revealed that enzymes have static heterogeneity of catalytic activity.^{22–26,28,29}

As more is known about the functional substates of enzymes, it has been increasingly recognized that functional substates are a key for molecular mechanisms of enzyme functions^{15–28} as well as evolutionary dynamics for the acquisition of new functions.^{4,30–33} Specifically, functional substates have been proposed to underlie enzyme promiscuity (or multi-functionality); within an ensemble of molecules, certain dominant functional substates can exclusively perform the native function, whereas some minor functional substates catalyze secondary or promiscuous reactions.^{4,30–33} Thus, it is postulated that the evolutionary optimization of enzyme function occurs by shifting the population balance among functional substates and that enzymes with well-optimized native activities have become specialists throughout evolution by converging toward a limited number of functional substates.^{4,30–33} In this view, functional substates of enzymes arise not only from conformational ensembles of native- or near-native forms but also from metastable conformational states trapped during folding and maturation processes such as proline isomerization or disulfide bond formation.^{30,34,35}

Received: June 25, 2022

Published: January 27, 2023



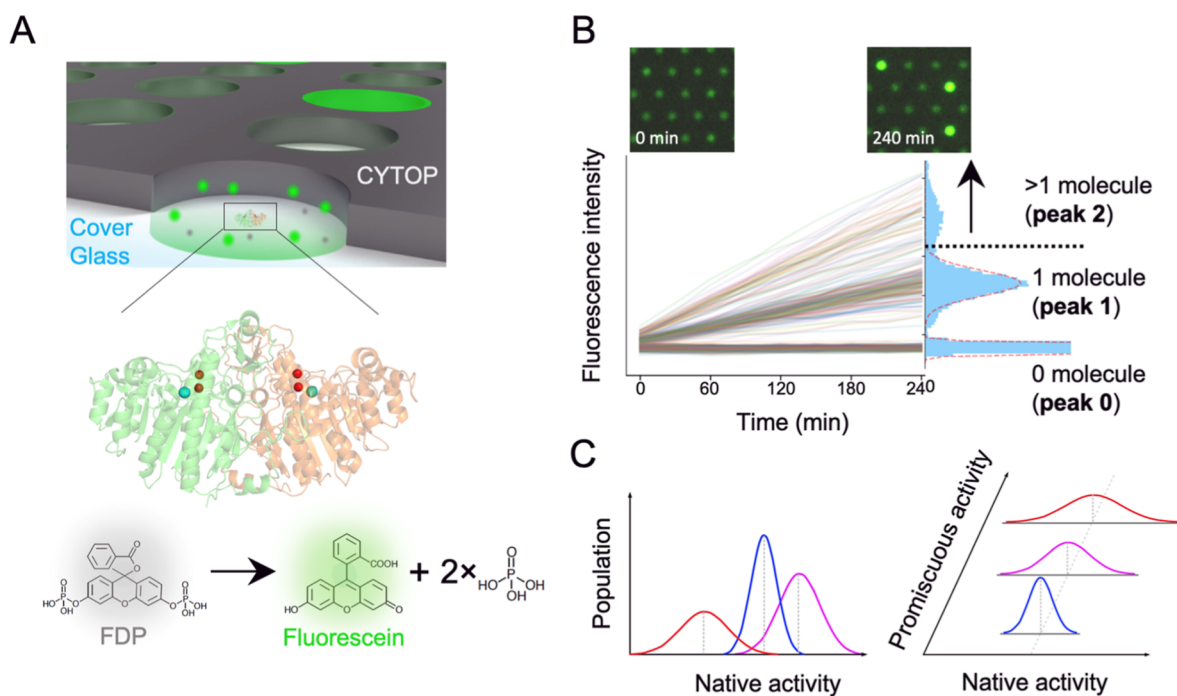


Figure 1. FRAD for measuring single enzyme activity. (A) Schematic image of the single-molecule assay in the FRAD. In each well or “reactor” patterned on amorphous perfluoro polymer (CYTOP), a single AP molecule hydrolyzes non-fluorescent FDP substrate molecules to release fluorescent product molecules (fluorescein), which accumulate in the reactor. Red and magenta spheres in the crystal structure of dimeric AP-wt (PDB ID: 1ED8) represent Zn^{2+} and Mg^{2+} ions in the active site. (B) Typical time-course measurement of fluorescence intensity in reactors. Time-course images were obtained at 20 min intervals for 240 min. The histogram shows the distribution of fluorescence intensity at 240 min. The histogram typically presents three peaks: peak 0 (enzyme-free reactors), peak 1 (single enzyme activity), and peak 2 (containing two or more enzyme molecules in a single reactor). The dotted red and black lines indicate fitting with Gaussian functions and threshold to exclude peak 2 from the analysis. The top panels exhibit snapshots of time-course measurements of catalytic activities observed by microscopy. Reactors containing AP-wt molecules exhibit an increase in fluorescence intensity. (C) Illustration of the aims of this study. The first aim is to investigate how readily single-point mutations modulate functional substates (left). The second aim is to evaluate possible correlation between variance of the native activity and promiscuous activity (right).

The above contention suggests that mutations can perturb the conformational substates and resultantly functional substates optimized for the native activity, regaining promiscuous functions. Hence, manipulating the functional substate by mutation is a key approach to understanding enzyme evolution and also harnessing promiscuous activities for enzyme engineering.³⁰ It has been shown that the gaining of promiscuous activity by mutations accompanies the enhancement of conformational heterogeneity.^{31,36} In this regard, Gorris and co-workers reported an implicative result.²³ They measured catalytic activities of the partially evolved β -glucuronidase (GUS) with high promiscuous activity at a single-molecule level by the use of a microreactor array device. They found that the partially evolved enzyme showed significantly higher heterogeneity of the catalytic activities than wild-type enzyme. This finding is supportive of the above-mentioned concept of enzyme evolution. However, such approaches have applied to only a handful of systems with a limited number of variants. Thus, many fundamental questions concerning functional substates remain elusive. Has evolution enriched specific functional substates during the functional optimization of natural enzymes? How easily can mutations modulate functional substates?

In this study, we aim to address these questions in a more comprehensive approach by use of *Escherichia coli* (*E. coli*) alkaline phosphatase (AP) that form a homodimer. We prepared wild-type and 69 mutants with single-point mutation across the whole structure of AP and measured molecule-to-

molecule heterogeneity of catalytic activity with FRAD. It is known that AP can show a stable functional substate originating from a heterodimer with a monomer deficient in Zn^{2+} incorporation or disulfide bond formation.²⁸ Considering that such a stable conformational state is also one of the molecular mechanisms to gain functional substates and possibly promiscuous activities, we analyzed the functional substates including the heterodimer fraction. The result showed that functional substates of AP can be readily altered by a single-point mutation from relatively homogeneous functional substates of the wild-type AP (AP-wt). We also tested potential correlations involving expansion of the functional substates and promiscuity by measuring the catalytic activity of mutants displaying the different extent of functional substates against various promiscuous substrates. Finally, we discussed the contribution of molecule-to-molecule heterogeneity to enzyme promiscuity and its evolution.

RESULTS AND DISCUSSION

Single-Molecule Assay of *E. coli* AP. We employed *E. coli* AP as a model to characterize the functional substates. AP is a homodimeric metalloenzyme encompassing two Zn^{2+} ions and one Mg^{2+} in its active site (Figure 1A). AP was expressed using the PURE system, a reconstituted cell-free protein synthesis system optimized in our previous studies.^{28,37} After AP molecules were expressed, the PURE reaction solution was diluted and mixed with a fluorescein-based fluorogenic

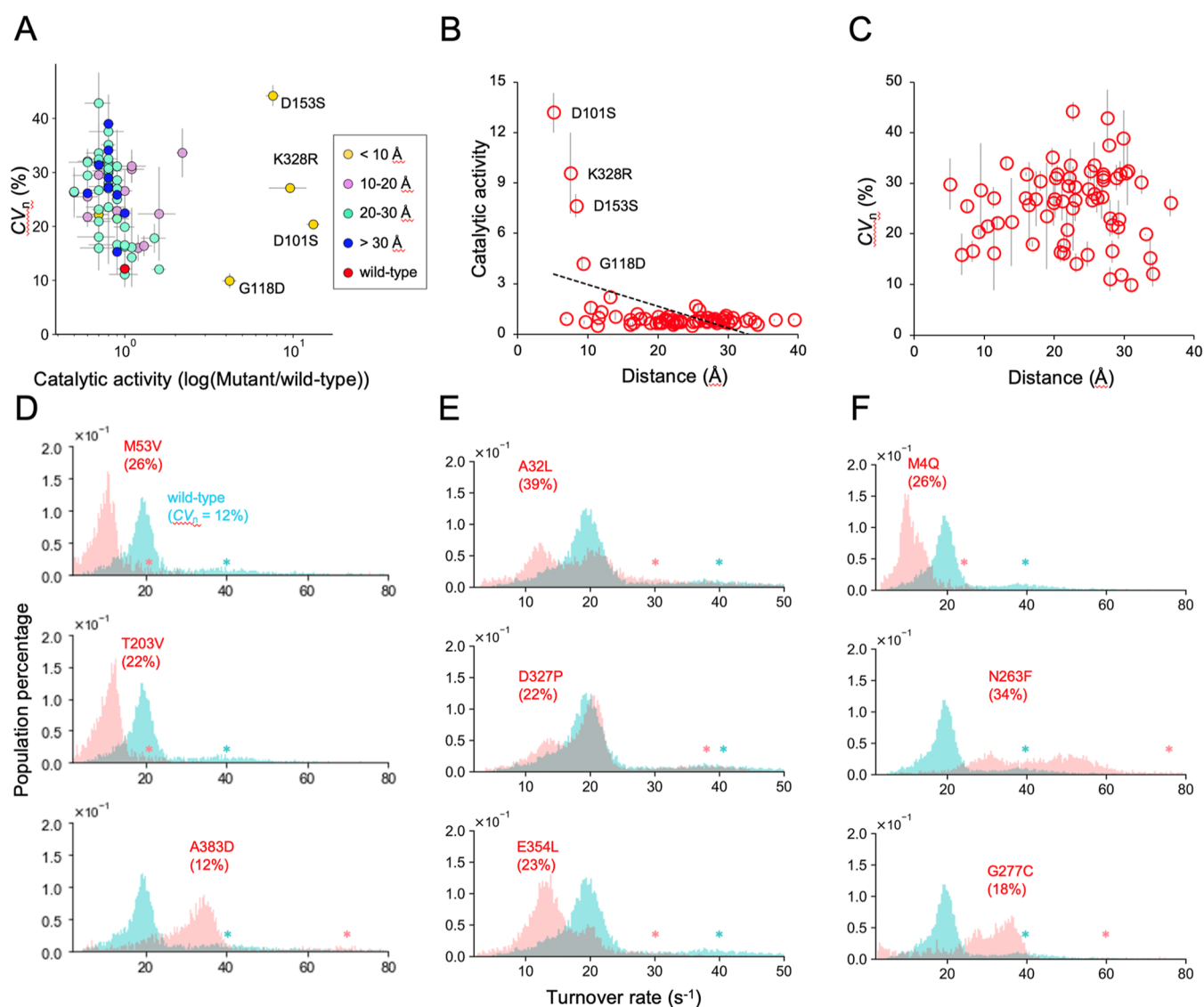


Figure 2. Alteration in catalytic activity and functional substates by single-point mutations. (A) Catalytic activity and functional substates (CV_n) (%) of AP-wt and mutant APs were plotted (means \pm SD). The turnover rate of the mutants was normalized to that of the AP-wt, and the x -axis was converted to a logarithmic scale. The data points are colored according to the distance (\AA) between a given mutation and the ligand (phosphate) present in the active site to the crystal structure of AP. The red-filled circle represents the AP-wt. (B) Dependence of activity on distance from the ligand to mutation sites. The turnover rate of the mutants was normalized to that of the AP-wt. The dotted line shows a linear fitting of the plot (slope = -0.13 , $R^2 = 0.24$). (C) Dependence of CV_n on the distance from ligand to mutation sites. (D–F) Representative distributions of mutants that exhibited single peaks shifted from the AP-wt (D), additional peaks partially overlapping with the AP-wt (E), and shifted additional peaks (F). The population of double occupancy of enzyme molecule (peak 2) was shown with cyan (AP-wt) and red (mutants) asterisks. The total number of enzyme molecules was higher than 1000.

phosphate monoesters substrate (fluorescein diphosphate, FDP) (Figure 1A). Subsequently, to measure single enzyme activity, the enzyme assay mixture was applied to a flow channel of the FRAD displaying over 46,000 reactors (Figures 1A and S1). A fluorinated oil (FC-40) was then injected into the flow channel to displace the enzyme assay mixture and seal the reactors (Figure S1). Note that our previous work confirmed that the catalytic activity of AP can be quantitatively measured using a FRAD by simple dilution with assay solution; no obvious effect of components brought in by the PURE system was observed through repeated single-molecule assays after buffer exchange with PURE-free solution.^{28,38} We also assessed possible cross-reactor diffusion between reactors via solution leakage by the photobleaching experiment. The fluorescein dye was encapsulated in the reactors, and one

reactor was photobleached by laser irradiation (Figure S2A). Fluorescence intensity in the photobleached reactor was not recovered and surrounding reactors did not significantly change for 4 h, ensuring negligible cross-reactor diffusion levels throughout the experiment (Figure S2B). The single enzyme activity was measured by the increase in the fluorescence intensity in the reactors (top panels in Figure 1B). The single-molecule assay was performed according to previously optimized reaction conditions using 1 mM FDP because AP exhibits catalytic activity even after 6 h without any significant decrease in activity.²⁸

Functional Substates of Wild-Type AP. The catalytic activities and functional substates among AP-wt molecules were evaluated based on the distribution of fluorescence intensity observed in all reactors (Figure 1B). The histograms

of fluorescence intensity typically showed two main discrete peaks: a peak of low fluorescence intensity was derived from enzyme-free reactors (peak 0) and another (peak 1) with higher fluorescence intensity represents reactors containing a single enzyme molecule. We occasionally observed an additional peak (peak 2) containing two or more enzyme molecules, which exhibited approximately two-fold higher intensity than peak 1.^{24,28} Peak 1 corresponded with the existence of multiple long-lived functional substates because AP-wt exhibited a linear increase of the fluorescence signal over time observed in earlier studies (Figures 1B and S3A).^{24,28} After identifying enzyme activities, the increase rate in fluorescence intensity (a.u./min) was calculated (see Methods), and then, the increase rate was converted into the turnover rate (s^{-1}) by using the fluorescence calibration curve (Figure S4A). Peak 2 derived from double occupancy of enzyme molecules was identified based on Poisson statistics (eq 1 in Methods) and excluded from the analysis (see Methods). Note that the enzyme solution was largely diluted to reduce the population of peak 2 reactors in all measurements. The mean turnover rate (MT_1) and standard deviation (SD_1) were calculated by fitting the distribution with a single Gaussian function. The mean catalytic activity of the AP-wt was determined to be 19.2 ± 1.3 (s^{-1}), consistent with the turnover rate determined in bulk measurement, $27 s^{-1}$ (Figures S3B and S4C). The concentration of FDP in the single-molecule assay was sufficiently higher than the K_m obtained in bulk measurements ($K_m = 8 \mu M$) for AP-wt (Figure S3A,B) and a mutant (D101S, $K_m = 419 \mu M$) in an earlier study.²⁸ Heterogeneity in catalytic activities was defined as the coefficient of variation ($CV_1 = 100 \times SD_1/MT_1$, %). The CV of AP-wt (CV_1 for peak 1 = $14 \pm 2\%$ in four independent measurements) was approximately two-fold higher than the inherent noise of the measurement determined from the CV of peak 0 ($CV_0 = 7 \pm 1\%$) (see Methods). Finally, we calculated the “functional substates” of AP-wt as the normalized CV (CV_n) by compensating for system noise, CV_0 , as

$$CV_n = \sqrt{CV_1^2 - CV_0^2} \quad (1)$$

The resulting CV_n for AP-wt was $12 \pm 3\%$. This value is fundamentally consistent with that of CV_n , $10 \pm 4\%$ for AP-wt purified after expression in *E. coli*,²⁸ ensuring the validity of the dilution protocol after cell-free expression.

Functional Substates of Single-Point Mutants. To investigate whether the functional substates can be modulated by mutations (left figure in Figure 1C), we randomly selected 65 single-point mutants of *E. coli* AP from a mutagenized library that we previously generated.³⁷ In addition, we prepared four mutants (D101S, G118D, D153S, and K328R) that were identified as highly active clones against FDP (see Methods). In total, 69 mutants were examined by single-molecule assay with FRAD. The activity of each mutant was measured in duplicate, and turnover rate (s^{-1}) and functional substates (CV_n , %) in the distribution of turnover rate were analyzed. Variations in the functional substates were observed, as the single enzyme peak (peak 1) could represent a single peak or comprise two neighboring peaks, for example, E66V and S245E (Figure S5). Such bimodal distributions were discriminated from double occupancy of enzyme molecules in a single reactor based on Poisson statistics (see Methods and Figure S6). The bimodal distributions are not attributable to the dynamic equilibrium of dimer and monomer of AP because

the monomeric form of AP significantly reduced activity to below detection limit of FRAD (see Table S1).⁴⁴ In addition, the dimer complex of AP-wt was shown to be stable under the condition of single-molecule assays with FRAD. We investigated the dimer stability of several mutants, by testing the dilution effect. The bimodal distribution did not change even under diluted conditions, ensuring that mutant enzymes also existed as a monodisperse dimer complex in reactors.²⁸ Including mutants of bimodal distributions, we determined CV values for all mutants by fitting them with a single Gaussian function. This is to maintain the uniformity of analysis and also because there was no noticeable difference in CV values between single or double Gaussian fitting (Figure S7). Catalytic activity was determined by end-point measurement. The replicates for all mutants exhibited good reproducibility in determining catalytic activity and CV_n (Figure S8). Note that the monotonous increment of signal means that the functional substates of AP enzymes were stable over hours without obvious transitions between other functional substates in consistent with previous studies (Figure 1B and see Methods).^{22–25,28,38} Regarding this point, one may concern that there is a rapid equilibrium among more detailed substates composing the functional substates. This is highly likely considering previous reports on dynamic disorder.^{17,23} At the same time, however, it is noteworthy that functional subsets as ensemble averages of such detailed substates are long-lived and differ from molecule to molecule.

Most randomly chosen mutations only marginally affected catalytic activity; almost all mutants presented a turnover rate within two-fold of the wild-type (Figure 2A). Furthermore, the 65 randomly selected mutants did not reveal any clear correlation between catalytic activity and the distance of the mutated site from the catalytic reaction center (Figure 2A,B). This is in contrast to the highly active mutants: D101S, G118D, D153S, and K328R which exhibited 4- to 13-fold higher activity than AP-wt (yellow symbols in Figure 2A). These mutations are located around the catalytic center (within 10 Å from the ligand).

We found that the AP-wt exhibited a single narrow distribution peak (Figures 2D–F, S5, and S9), its CV_n being one of the lowest among all mutants ($CV_n = 12\%$), which suggests that AP-wt exhibits highly homogeneous functional substates. Most mutants showed significantly broader distribution than the AP-wt, indicating that genetic perturbation expands the functional substates. On average, the CV_n of mutants was three-fold higher (26%), and some mutants showed close to four-fold higher CV_n than the AP-wt. Intriguingly, there was no apparent correlation between the CV_n and catalytic activity (Figure 2A). This observation suggests that the degree of functional substates is principally independent of the level of catalytic activity and that the molecular mechanism for expanding functional substates differs from that for catalysis enhancement. Across all mutants, we observed a broad range of combinations between functional substates and catalytic activity (Figures 2D–F and S9). Indeed, some mutants exhibited a single peak, yet displayed catalytic activities different from the wild-type (Figure 2D). We hypothesized that, in these specific cases, the mutation likely modulates the transition states of the kinetic bottleneck steps without disturbing the populations of functional substates. By contrast, in other mutants, one population exhibited catalytic activity comparable to that of the AP-wt (Figure 2E), and an additional population was also found, resulting in a bimodal

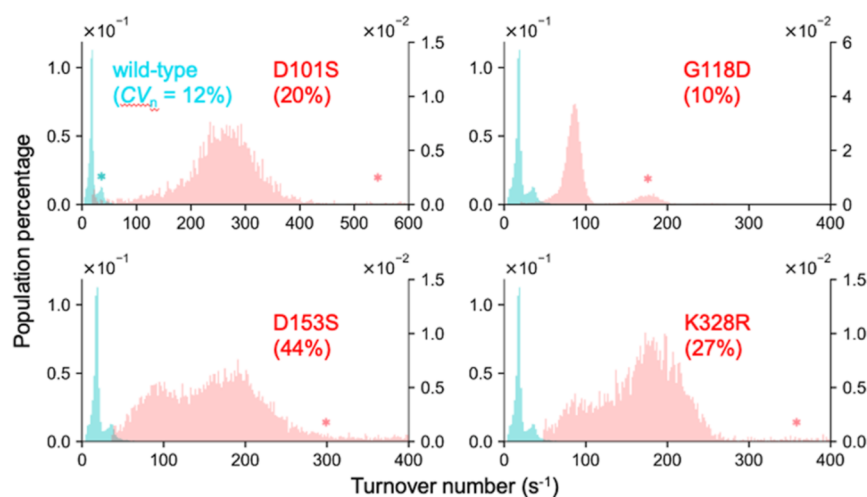


Figure 3. Alteration of catalytic activity and functional substrates in highly active mutants. Cyan and red bins show the distribution of the AP-wt (first y-axis) and mutants (second y-axis), respectively. Population of double occupancy of enzyme molecule (peak 2) was shown with cyan (AP-wt) and red (mutants) asterisks. The total number of enzyme molecules was higher than 1000.

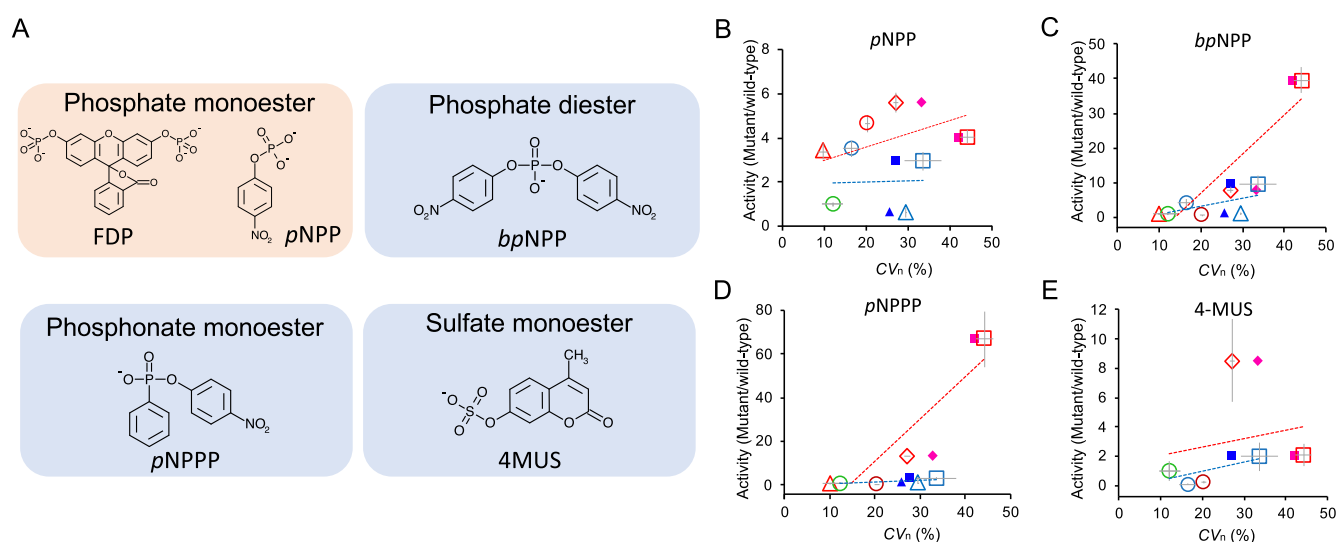


Figure 4. Correlation between functional substrates and promiscuous activity. (A) Chemical structures of phosphate monoesters (*p*-nitrophenyl phosphate, *p*NPP), phosphate diesters (bis-*p*-nitrophenyl phosphate, *bp*NPP), phosphonate monoesters (*p*-nitrophenyl phenyl phosphonate, *p*NPPP), and 4-methylumbelliferyl sulfate substrates. (B–E) Correlation between activities against those substrates and CV_n . The activity of mutant AP was comparable to that of AP-wt. The CV_n of the mutants was measured using the FDP shown in Figure 2. The green circle shows AP-wt, and red and blue plots exhibit that the distance of the mutation site from the active center is less or greater than 10 Å. Different forms of the plots indicate mutants; red circle (D101S), triangle (G118D), rectangular (D153S), diamond (K328R), and light blue circle (A119T), triangle (L196V), and rectangular (N263F). For the mutants with distinct bimodal distribution (D153S, K328R, L196V, and N263F), the data were also fitted with a double Gaussian function to determine CV_n represented in filled symbols. The linear approximation of data points in red symbols or blue ones provided fitting slopes; 0.06 ($R^2 = 0.24$) and -0.01 (0.003) in (B), 1.13 (0.86) and 0.23 (0.34) in (C), 1.93 (0.86) and 0.07 (0.40) in (D), and 0.06 (0.04) and 0.06 (0.59) in (E), respectively. T59R, G118D, A119T, or L196V was excluded from (B–E), (E), (D), or (E) because the mutants did not exhibit measurable activity against the substrates (see Table S1).

distribution. Mutations that lead to shifts between subpopulations, visible through the activity change in the ensemble average of enzymes, can underlie the emergence of new functional substrates within a clonal population. Such mutations may act to stabilize functional substrates, which were minor in the AP-wt. Finally, another set of mutations resulted in two peaks, although both peaks were shifted from that of the AP-wt population (Figure 2F), suggesting that these mutations can simultaneously modulate enzyme kinetics and the population balance between various functional substrates. Taken together, these observations suggest that a mutation can easily alter the balance of AP functional substrates, and the

effect on the population balance differs widely, depending on the specific mutation.

The four highly active AP mutants (D101S, G118D, D153S, and K328R) also exhibited distinct differences in terms of the diversification of functional substrates (Figure 3). D101S, D153S, and K328R exhibited shifted and broader distributions than the AP-wt. Especially, D153S showed the highest CV_n among the mutants. However, G118D showed a distribution similar to AP-wt despite having four-fold higher catalytic activity than the AP-wt. Thus, similar to the single-point mutants, wide variation in the functional substrates was observed among the highly active mutants. These significantly

heterogeneous functional substates in the highly active mutants might be due to structural heterogeneity involving the active site, such as the flipping of catalytically important residues or a large change in phosphate coordination as demonstrated by previous studies.^{39–42} In the future, further elucidation of the direct correlation between structural changes in the active site and the alteration of functional substates is pivotal to our understanding of enzyme mechanism and evolution.

Functional Substates and Structural Position of Mutations. To investigate whether AP possesses mutational hot spots that may be responsible for enhanced activity and/or functional substates, we plotted the catalytic activity and CV_n of every single mutation against the distance of Ca of mutation sites from phosphate in the active site (Figure 2B,C). We also presented a heat map of the crystal structure of AP-wt to map mutation sites with higher catalytic activity and CV_n on the 3D structure (Figure S10). Interestingly, the mutations giving rise to highly active mutants were located in the vicinity of the active site; however, there was no significant correlation between the CV_n and the distance from the active site. We also analyzed mutations based on their proximity to the two disulfide bonds (C168–C178 and C286–C336) or the interface between the monomers (Figure S11),^{43,44} but there were no clear correlations. Thus, these findings suggest that functional substates can potentially be modulated globally across the whole enzyme structure.

Functional Substates and Promiscuity. It has been suggested that the expansion of functional substates may be related to the enhancement of reactivity to promiscuous substrates.^{4,23,30–33} Thus, we purified AP-wt and seven mutants (D101S, G118D, A119T, D153S, L196V, N263F, and K328R) with different CV_n (10–44%) and mutation sites from phosphate (5–19 Å). Then, we analyzed the correlation between CV_n and catalytic activity against promiscuous substrates (right figure in Figure 1C): phosphate diesters (bis-*p*-nitrophenyl phosphate, *bp*NPP) and its analogue (*p*-nitrophenyl phenyl phosphonate, *p*NPPP) and sulfate monoesters (4-methylumbelliferyl sulfate, 4-MUS) in addition to another phosphate monoesters substrate, *p*-nitrophenyl phosphate (*p*NPP) for comparison purpose (Figure 4A). The activities against *bp*NPP, *p*NPPP, and 4-MUS were too low to be measured at the single-molecule level; hence, we measured their promiscuous activities in a bulk solution with purified enzymes (Figure S3C). A native phosphate monoesters substrate, *p*NPP, behaves similarly to FDP (Figure S3D), which did not show a correlation to CV_n (Figure 4B). AP-wt showed low but distinct promiscuous activities against *bp*NPP, *p*NPPP, and 4-MUS as it was shown in previous studies (Table S1).^{45–47} To confirm that the observed promiscuous activity is derived from the activity of AP-wt, we measured the activity of a monomeric AP mutant (T59R).⁴⁴ T59R, which exhibited 1000-fold low activity against *p*NPP than AP-wt, did not show detectable promiscuous activities, indicating that AP-wt catalyzed the promiscuous reactions. Intriguingly, positive correlations between CV_n and promiscuous activity against *bp*NPP and *p*NPPP were observed in the mutants with mutations in the active site (D101S, G118D, D153S, and K328R; red circles in Figure 4C,D) ($R^2 = 0.86$ for both plots). Note that because D153S and K328R showed bimodal distributions, their CV values were also determined by double Gaussian fitting (closed red rectangular and diamond in Figure 4B–E). The positive correlations between CV_n and promiscuous activity were still observed ($R^2 = 0.71$ and 0.72 for

Figure 4C,D). On the other hand, the positive correlations could hardly be observed in the mutants with mutation outside the active site (blue triangles in Figure 4C,D). For promiscuous activity against 4-MUS, positive correlations were not observed for all mutants (Figure 4E). Thus, these results indicated that the expansion of functional substates caused by a mutation close to the active site could increase activity for particular promiscuous substrates.

Genetic Perturbation Expands Functional Substates of AP-wt. In the present study, we assessed the functional substates of a model enzyme using AP-wt and 69 mutants by performing high-throughput single-molecule assays with the FRAD. AP-wt showed highly homogeneous functional substates, and most of the mutants showed multiple substates with various types. These observations showed that even a single-point mutation in AP-wt is prone to expanding functional substates, suggesting that AP-wt is perhaps optimized to reduce functional substates throughout evolution. A possible scenario is that AP has evolved as a specialist enzyme, minimizing the functional substates toward its native function of phosphate monoesterase. Native enzymes have undergone a long evolutionary process under various selection pressures from diverse environmental conditions; thus, these natural enzymes may have undergone optimization in terms of their conformational and functional substates.^{4,30–33} If the functional substates of AP-wt for its native function have been evolutionarily optimized over billions of years, mutations may readily disrupt the fine-tune balance of the substates. As a result, the expansion of the functional substates may lead to high heterogeneity in catalytic activities in most mutants independent of the level of catalytic activity toward FDP or *p*NPP (Figures 2A and 4B).

Regarding the diverse functional substates, one may argue the possible effect on the functional substates by surface adhesion of AP molecules. However, this is highly unlikely for two reasons. The first reason is that the degree of functional substates was very different for each mutant. It would be difficult to explain such diverse activity distribution seen in each mutant solely by the effects of the reactor surface. Second, most enzyme molecules were not adsorbed to the reactor surface. We have performed solution exchange experiments, which resulted in the loss of enzyme molecules from more than 90% of the reactors (Figure S12). Considering the re-encapsulation possibility, it is reasonable to assume that surface adsorption does not occur for the majority of molecules.

Evolution of Enzyme Function and Functional Substates. Does the expansion in functional substates measured by the single-molecule assay correlate with an increase in catalytic promiscuity? To test this, we measured promiscuous activity by using phosphodiester and sulfate monoesters substrates. One of the significant findings is that while mutation around the active site exhibited a correlation between functional substates and promiscuity, mutation outside the active site did not show clear correlations (Figure 4C,D). Similarly, in a previous study, evolved GUS with high promiscuous activity against several glycosidic substrates and mutations around the active site exhibited more extensive heterogeneity in catalytic activities than the wild-type enzyme.²³ Moreover, several studies have reported that mutations close to the active center significantly alter enzyme function.^{4,48,49} Thus, enzymes that exhibited highly heterogeneous functional substates with mutations in the active site

might have increased conformational substates for catalysis with multiple substrates. Considering that such expansion of functional substate would accompany the diversification of kinetics of catalysis, it is likely that the mutants of AP with high CV_n and high promiscuity have some functional substates with largely different kinetic features such as a different rate-limiting step. As for the mutants with mutation outside the active site, the heterogeneous functional substates would be derived from disruption of disulfide bonds, proline isomer, dimer interface, or different metal coordinations.^{28,43,44} Actually, AP molecules with deficiencies of disulfide bonds and metal state exhibited high and low active peaks derived from fully active dimer and half-active heterodimer formation.²⁸ Although all enzymes were expressed under the condition that fully active molecules are preferentially expressed by the supplement, there would be a possibility that the mutation changes metal and disulfide bond coordination, resulting in a bimodal distribution in catalytic activities shown in Figures 2E,F and 3. To grasp global trends of the mutational effect on the functional substates, we quantified the functional substates including the metastable population such as the heterodimer fraction that is trapped during folding, maturation processes due to unformed disulfide bond, deficiency of Zn^{2+} incorporation, and proline isomer. Because in the course of enzyme evolution to acquire novel functions, the selection pressure does not preferentially act on the most stable conformational population but also molecular population in kinetically trapped metastable conformational states.^{30,34,35} Indeed, we found a correlation between the functional substates and promiscuity with this definition (Figure 4).

Another important finding of this study is that while a significant positive correlation was observed between activity against the phosphate diester substrates and CV_n , activity against sulfate monoesters substrate did not show the correlation (Figure 4E). This indicates that the expanded functional substates against FDP may not be involved in the catalysis of the sulfate monoester substrate. In fact, despite the sulfate monoester substrate showing a similar chemical structure to the phosphate monoester substrate, AP and sulfatase are known to be highly selective for these substrates.^{46,47} The high selectivity is thought to be derived from different active site structures. Sulfatase exploits one divalent metal and formylglycine which needs posttranslational activation for the catalysis.^{46,47} However, AP has two Zn^{2+} and one Mg^{2+} in the active site. Therefore, the active site structure of sulfatase is distinct from AP. Moreover, the bi-metallo core of AP is similar to that of nucleotide pyrophosphatases/phosphodiesterases (NPPs), which catalyzes phosphate diester substrates including *bp*NPP and exhibits catalytic promiscuity for the phosphate monoester substrate.^{47,50} Therefore, based on the similarity of the structure and reaction between AP and NPP, the high functional substates against FDP might include substates that react with phosphodiester substrates, and thus, the positive correlations between CV_n and phosphodiesterase activity were observed.

These findings and our results reinforce the long-discussed concept of enzyme evolution; enzymes can enhance their promiscuity or multi-functionality by expanding functional substates. However, the correlation between the functional substates and the conformational substates, especially around the active site,^{51–53} has not yet been known. Because the mutations that enhanced functional substates in this study were not only localized around the active site but across the

whole enzyme structure, the effect of remote mutations may also need to be included in the analysis of the correlation. Moreover, only a handful of enzymes and their variants have been measured at the level of single enzyme kinetics to date, and it is difficult to generalize these observations to other systems. For further generalization of this scenario, more comprehensive studies involving the various types of enzymes and kinetic/structural analysis are required.

CONCLUSIONS

In this study, we investigated the effect of genetic perturbation on functional substates by a single-molecule assay using FRAD. The results showed that AP-wt exhibited the highest homogeneous functional substates among the mutants, but single-point mutation across the whole enzyme structure significantly expanded the substates of AP-wt. Moreover, highly heterogeneous functional substates were correlated with high catalytic promiscuity. Thus, our findings indicate that even enzymes that have acquired high specificity, such as the wild-type enzyme, can again acquire catalytic promiscuity by expanding functional substates through genetic perturbations. These properties of enzymes would contribute to the adaptation of organisms to their ever-changing environment.

ASSOCIATED CONTENT

Supporting Information

The Supporting Information is available free of charge at <https://pubs.acs.org/doi/10.1021/jacs.2c06693>.

Kinetic data of the single-molecule assay (XLSX)

Materials and methods, setup of FRAD for the single-molecule assay, inspection of possible cross-reactor diffusion of fluorescein dye by photobleaching experiment, characterization of catalytic activity of APs in FRAD and bulk solution, linear correlation between fluorescein dye concentration and fluorescence intensity, distribution of catalytic activities measured with FRAD, double Gaussian fittings of the distribution of enzyme activities, effect of single and double Gaussian fittings on CV, quality of single-molecule assays with FRAD, comparison of distribution of catalytic activities among AP-wt and mutants, magnitude of effect of mutation on catalytic activity and functional substates, effects of mutations in catalytic activity and functional substates on functionally important sites on AP, solution exchange experiment of AP-wt, and catalytic activity of AP-wt and mutants in bulk solution (PDF)

AUTHOR INFORMATION

Corresponding Authors

Nobuhiko Tokuriki – Michael Smith Laboratories, The University of British Columbia, British Columbia V6T1Z4, Canada; orcid.org/0000-0002-8235-1829; Email: nobuhiko.tokuriki@ubc.ca

Hiroyuki Noji – Department of Applied Chemistry, The University of Tokyo, Tokyo 113-8656, Japan; orcid.org/0000-0002-8842-6836; Email: hnoji@g.ecc.u-tokyo.ac.jp

Authors

Morito Sakuma – Department of Applied Chemistry, The University of Tokyo, Tokyo 113-8656, Japan; Michael Smith Laboratories, The University of British Columbia, British

Columbia V6T1Z4, Canada; orcid.org/0000-0002-8804-9831

Shingo Honda – Department of Applied Chemistry, The University of Tokyo, Tokyo 113-8656, Japan; Present Address: University of Washington, Seattle, Washington, 98195, United States; orcid.org/0000-0002-9403-6631

Hiroshi Ueno – Department of Applied Chemistry, The University of Tokyo, Tokyo 113-8656, Japan

Kazuhito V. Tabata – Department of Applied Chemistry, The University of Tokyo, Tokyo 113-8656, Japan; orcid.org/0000-0002-0463-1374

Kentaro Miyazaki – International Center for Biotechnology, Osaka University, Suita 565-0871, Japan

Complete contact information is available at:
<https://pubs.acs.org/10.1021/jacs.2c06693>

Author Contributions

All authors have given approval to the final version of the manuscript.

Funding

This work was supported by the ImPACT Program of the Council for Science, Technology, and Innovation, Japan Science and Technology Agency (JST) (to H.N.), Grant-in-Aid for Scientific Research on Innovation Areas from the Japan Society for the Promotion of Science (JSPS) (JP19H05380 to H.U.), Grant-in-Aid for Scientific Research (S) from JSPS (JP19H05624 to H.N.), CREST program from JST, (JPMJCR19S4 to H.N.), and Human Frontier Science Program (HFSP) Program Grant (RGP0054/2020) (to H.N. and N.T.).

Notes

The authors declare no competing financial interest.

ACKNOWLEDGMENTS

The authors are grateful to Kenji Akama, Naoki Soga, and Mayu Hara for their measurement and technical assistance and to Toshiharu Suzuki and members of the Tokuriki lab for helpful discussions and revision of the paper.

ABBREVIATIONS

E. coli *Escherichia coli*
AP alkaline phosphatase
FRAD femtoliter reactor array device
CV coefficient of variation

REFERENCES

- (1) Frauenfelder, H.; McMahon, B. H.; Austin, R. H.; Chu, K.; Groves, J. T. The role of structure, energy landscape, dynamics, and allostery in the enzymatic function of myoglobin. *Proc. Natl. Acad. Sci. U.S.A.* **2001**, *98*, 2370–2374.
- (2) Henzler-Wildman, K.; Kern, D. Dynamic Personalities of Proteins. *Nature* **2007**, *450*, 964–972.
- (3) Boehr, D. D.; Nussinov, R.; Wright, P. E. The Role of Dynamic Conformational Ensembles in Biomolecular Recognition. *Nat. Chem. Biol.* **2009**, *5*, 789–796.
- (4) Khersonsky, O.; Tawfik, D. S. Enzyme Promiscuity: A Mechanistic and Evolutionary Perspective. *Annu. Rev. Biochem.* **2010**, *79*, 471–505.
- (5) Luo, X.; Tang, Z.; Xia, G.; Wassmann, K.; Matsumoto, T.; Rizo, J.; Yu, H. The Mad2 Spindle Checkpoint Protein Has Two Distinct Natively Folded States. *Nat. Struct. Mol. Biol.* **2004**, *11*, 338–345.
- (6) Tuinstra, R.; Peterson, F.; Kutlesa, S.; Elgin, E. S.; Kron, M.; Volkman, B. Interconversion between Two Unrelated Protein Folds

in the Lymphotactin Native State. *Proc. Natl. Acad. Sci. U.S.A.* **2008**, *105*, 5057–5062.

(7) Skinner, J. J.; Wood, S.; Shorter, J.; Englander, S. W.; Black, B. E. The Mad2 Partial Unfolding Model: Regulating Mitosis through Mad2 Conformational Switching. *J. Cell Biol.* **2008**, *183*, 761–768.

(8) Alexander, P. A.; He, Y.; Chen, Y.; Orban, J.; Bryan, P. N. A Minimal Sequence Code for Switching Protein Structure and Function. *Proc. Natl. Acad. Sci. U.S.A.* **2009**, *106*, 21149–21154.

(9) Bryan, P. N.; Orban, J. Proteins That Switch Folds. *Curr. Opin. Struct. Biol.* **2010**, *20*, 482–488.

(10) Ramanathan, A.; Savol, A.; Burger, V.; Chennubhotla, C. S.; Agarwal, P. K. Protein Conformational Populations and Functionally Relevant Substates. *Acc. Chem. Res.* **2014**, *47*, 149–156.

(11) Agarwal, P. K.; Doucet, N.; Chennubhotla, C.; Ramanathan, A.; Narayanan, C. Conformational Sub-States and Populations in Enzyme Catalysis. *Methods Enzymol.* **2016**, *578*, 273–297.

(12) Si, Z.; Zhang, J.; Shivakoti, S.; Atanasov, I.; Tao, C. L.; Hui, W. H.; Zhou, K.; Yu, X.; Li, W.; Luo, M.; Bi, G. Q.; Zhou, Z. H. Different Functional States of Fusion Protein GB Revealed on Human Cytomegalovirus by Cryo Electron Tomography with Volta Phase Plate. *PLoS Pathog.* **2018**, *14*, No. e1007452.

(13) Dishman, A. F.; Tyler, R. C.; Fox, J. C.; Kleist, A. B.; Prehoda, K. E.; Babu, M. M.; Peterson, F. C.; Volkman, B. F. Evolution of Fold Switching in a Metamorphic Protein. *Science* **2021**, *371*, 86–90.

(14) Petrie, K. L.; Palmer, N. D.; Johnson, D. T.; Medina, S. J.; Yan, S. J.; Li, V.; Burmeister, A. R.; Meyer, J. R. Destabilizing mutations encode nongenetic variation that drives evolutionary innovation. *Science* **2018**, *359*, 1542–1545.

(15) Sohl, J.; Jaswal, S.; Agard, D. Unfolded conformations of α -lytic protease are more stable than its native state. *Nature* **1998**, *395*, 817–819.

(16) Xue, Q.; Yeung, E. S. Differences in the chemical reactivity of individual molecules of an enzyme. *Nature* **1995**, *373*, 681–683.

(17) Lu, H. P.; Xun, L.; Xie, X. S. Single-Molecule Enzymatic Dynamics. *Science* **1998**, *282*, 1877–1882.

(18) Craig, D. B.; Dovichi, N. J. *Escherichia coli* β -Galactosidase Is Heterogeneous with Respect to the Activity of Individual Molecules. *Can. J. Chem.* **1998**, *76*, 623–626.

(19) Hirono-Hara, Y.; Noji, H.; Nishiura, M.; Muneyuki, E.; Hara, K. Y.; Yasuda, R.; Kinosita, K.; Yoshida, M. Pause and Rotation of F1-ATPase during Catalysis. *Proc. Natl. Acad. Sci. U.S.A.* **2001**, *98*, 13649–13654.

(20) Dyck, A. C.; Craig, D. B. Individual Molecules of Thermostable Alkaline Phosphatase Support Different Catalytic Rates at Room Temperature. *Luminescence* **2002**, *17*, 15–18.

(21) English, B. P.; Min, W.; van Oijen, A. M.; Lee, T. L.; Luo, G.; Sun, H.; Cherayil, B. J.; Kou, S. C.; Xie, X. S. Ever-Fluctuating Single Enzyme Molecules: Michaelis-Menten Equation Revisited. *Nat. Chem. Biol.* **2006**, *2*, 87–94.

(22) Rissin, D. M.; Gorris, H. H.; Walt, D. R. Distinct and Long-Lived Activity States of Single Enzyme Molecules. *J. Am. Chem. Soc.* **2008**, *130*, 5349–5353.

(23) Liebherr, R. B.; Renner, M.; Gorris, H. H. A Single Molecule Perspective on the Functional Diversity of in Vitro Evolved β -Glucuronidase. *J. Am. Chem. Soc.* **2014**, *136*, 5949–5955.

(24) Obayashi, Y.; Iino, R.; Noji, H. A Single-Molecule Digital Enzyme Assay Using Alkaline Phosphatase with a Coumarin-Based Fluorogenic Substrate. *Analyst* **2015**, *140*, 5065–5073.

(25) Mickert, M. J.; Gorris, H. H. Transition-State Ensembles Navigate the Pathways of Enzyme Catalysis. *J. Phys. Chem. B* **2018**, *122*, 5809–5819.

(26) Jiang, Y.; Li, X.; Morrow, B. R.; Pothukuchy, A.; Gollihar, J.; Novak, R.; Reilly, C. B.; Ellington, A. D.; Walt, D. R. Single-Molecule Mechanistic Study of Enzyme Hysteresis. *ACS Cent. Sci.* **2019**, *5*, 1691–1698.

(27) Galenkamp, N. S.; Biesemans, A.; Maglia, G. Directional Conformer Exchange in Dihydrofolate Reductase Revealed by Single-Molecule Nanopore Recordings. *Nat. Chem.* **2020**, *12*, 481–488.

- (28) Ueno, H.; Kato, M.; Minagawa, Y.; Hirose, Y.; Noji, H. Elucidation and Control of Low and High Active Populations of Alkaline Phosphatase Molecules for Quantitative Digital Bioassay. *Protein Sci.* **2021**, *30*, 1628–1639.
- (29) Noji, H.; Minagawa, Y.; Ueno, H. Enzyme-based Digital Bioassay Technology – Key Strategies and Future Perspective. *Lab Chip* **2022**, *22*, 3092–3109.
- (30) Tokuriki, N.; Tawfik, D. S. Protein Dynamism and Evolvability. *Science* **2009**, *324*, 203–207.
- (31) Ma, B.; Nussinov, R. Protein Dynamics: Conformational Footprints. *Nat. Chem. Biol.* **2016**, *12*, 890–891.
- (32) Petrović, D.; Risso, V. A.; Kamerlin, S. C. L.; Sanchez-Ruiz, J. M. Conformational Dynamics and Enzyme Evolution. *J. R. Soc., Interface* **2018**, *15*, 20180330.
- (33) Nussinov, R.; Tsai, C. J.; Jang, H. Protein Ensembles Link Genotype to Phenotype. *PLoS Comput. Biol.* **2019**, *15*, No. e1006648.
- (34) Kaplan, A. R.; Olson, R.; Alexandrescu, A. T. Protein Yoga: Conformational Versatility of the Hemolysin II C-Terminal Domain Detailed by NMR Structures for Multiple States. *Protein Sci.* **2021**, *30*, 990–1005.
- (35) Meier, S.; Jensen, P. R.; David, C. N.; Chapman, J.; Holstein, T. W.; Grzesiek, S.; Özbek, S. Continuous Molecular Evolution of Protein-Domain Structures by Single Amino Acid Changes. *Curr. Biol.* **2007**, *17*, 173–178.
- (36) Campbell, E.; Kaltenbach, M.; Correy, G. J.; Carr, P. D.; Porebski, B. T.; Livingstone, E. K.; Afriat-Jurnou, L.; Buckle, A. M.; Weik, M.; Hollfelder, F.; Tokuriki, N.; Jackson, C. J. The Role of Protein Dynamics in the Evolution of New Enzyme Function. *Nat. Chem. Biol.* **2016**, *12*, 944–950.
- (37) Zhang, Y.; Minagawa, Y.; Kizoe, H.; Miyazaki, K.; Iino, R.; Ueno, H.; Tabata, K. V.; Shimane, Y.; Noji, H. Accurate High-Throughput Screening Based on Digital Protein Synthesis in a Massively Parallel Femtoliter Droplet Array. *Sci. Adv.* **2019**, *5*, No. eaav8185.
- (38) Honda, S.; Minagawa, Y.; Noji, H.; Tabata, K. V. Multidimensional Digital Bioassay Platform Based on an Air-Sealed Femtoliter Reactor Array Device. *Anal. Chem.* **2021**, *93*, 5494–5502.
- (39) Chen, L.; Neidhart, D.; Kohlbrenner, W. M.; Mandecki, W.; Bell, S.; Sowadski, J.; Abad-Zapatero, C. 3-d Structure of a Mutant (Asp101 → Ser) of E.Coli Alkaline Phosphatase with Higher Catalytic Activity. *Protein Eng., Des. Sel.* **1992**, *5*, 605–610.
- (40) Dealwis, C. G.; Brennan, C.; Christianson, K.; Mandecki, W.; Abad-Zapatero, C. Crystallographic Analysis of Reversible Metal Binding Observed in a Mutant (Asp 153 → Gly) of Escherichia Coli Alkaline Phosphatase. *Biochemistry* **1995**, *34*, 13967–13973.
- (41) Murphy, J. E.; Tibbitts, T. T.; Kantrowitz, E. R. Mutations at Positions 153 and 328 in Escherichia Coli Alkaline Phosphatase Provide Insight towards the Structure and Function of Mammalian and Yeast Alkaline Phosphatases. *J. Mol. Biol.* **1995**, *253*, 604–617.
- (42) Sunden, F.; Peck, A.; Salzman, J.; Ressler, S.; Herschlag, D. Extensive Site-Directed Mutagenesis Reveals Interconnected Functional Units in the Alkaline Phosphatase Active Site. *Elife* **2015**, *4*, No. e06181.
- (43) Sone, M.; Kishigami, S.; Yoshihisa, T.; Ito, K. Roles of Disulfide Bonds in Bacterial Alkaline Phosphatase. *J. Biol. Chem.* **1997**, *272*, 6174–6178.
- (44) Boulanger, R. R.; Kantrowitz, E. R. Characterization of a Monomeric Escherichia Coli Alkaline Phosphatase Formed upon a Single Amino Acid Substitution. *J. Biol. Chem.* **2003**, *278*, 23497–23501.
- (45) O'Brien, P. J.; Herschlag, D. Functional Interrelationships in the Alkaline Phosphatase Superfamily: Phosphodiesterase Activity of Escherichia Coli Alkaline Phosphatase. *Biochemistry* **2001**, *40*, 5691–5699.
- (46) Mohamed, M. F.; Hollfelder, F. Efficient, Crosswise Catalytic Promiscuity among Enzymes That Catalyze Phosphoryl Transfer. *Biochim. Biophys. Acta, Proteins Proteomics* **2013**, *1834*, 417–424.
- (47) Pabis, A.; Kamerlin, S. C. L. Promiscuity and Electrostatic Flexibility in the Alkaline Phosphatase Superfamily. *Curr. Opin. Struct. Biol.* **2016**, *37*, 14–21.
- (48) Gould, S. M. Q.; Tawfik, D. S. Directed Evolution of the Promiscuous Esterase Activity of Carbonic Anhydrase II. *Biochemistry* **2005**, *44*, 5444–5452.
- (49) López-Canut, V.; Roca, M.; Bertrán, J.; Moliner, V.; Tuñón, I. Promiscuity in Alkaline Phosphatase Superfamily. Unraveling Evolution through Molecular Simulations. *J. Am. Chem. Soc.* **2011**, *133*, 12050–12062.
- (50) Sunden, F.; AlSadhan, I.; Lyubimov, A.; Doukov, T.; Swan, J.; Herschlag, D. Differential Catalytic Promiscuity of the Alkaline Phosphatase Superfamily Bimetallo Core Reveals Mechanistic Features Underlying Enzyme Evolution. *J. Biol. Chem.* **2017**, *292*, 20960–20974.
- (51) Yang, H.; Luo, G.; Karnchanaphanurach, P.; Louie, T. M.; Rech, I.; Cova, S.; Xun, L.; Xie, X. S. Protein Conformational Dynamics Probed by Single-Molecule Electron Transfer. *Science* **2003**, *302*, 262–266.
- (52) Kahsai, A. W.; Xiao, K.; Rajagopal, S.; Ahn, S.; Shukla, A. K.; Sun, J.; Oas, T. G.; Lefkowitz, R. J. Multiple Ligand-Specific Conformations of the B2-Adrenergic Receptor. *Nat. Chem. Biol.* **2011**, *7*, 692–700.
- (53) Jensen, S. B.; Thodberg, S.; Parween, S.; Moses, M. E.; Hansen, C. C.; Thomsen, J.; Sletfjerd, M. B.; Knudsen, C.; Del Giudice, R.; Lund, P. M.; Castaño, P. R.; Bustamante, Y. G.; Velazquez, M. N. R.; Jørgensen, F. S.; Pandey, A. V.; Laursen, T.; Møller, B. L.; Hatzakis, N. S. Biased Cytochrome P450-Mediated Metabolism via Small-Molecule Ligands Binding P450 Oxidoreductase. *Nat. Commun.* **2021**, *12*, 2260.